Analytical Methods

Accepted Manuscript

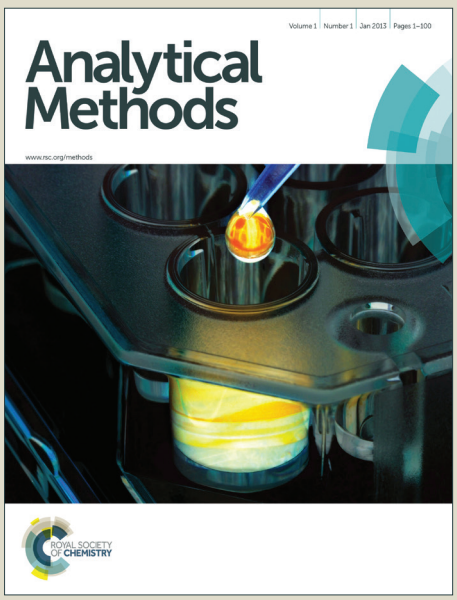

ROYAL SOCIETY OF CHEMISTRY

www.rsc.org/methods

Post Derivative TLC Densitometric Stability Indicating Assay for Mesterolone and Quantum Chemical Calculations

Syed Ghulam Musharraf[a*], Qamar ul Arfeen[a], Faraz Ul Haq[a] and Haris Ahmed[b],

[a]H.E.J. Research Institute of Chemistry, International Center for Chemical and Biological Sciences, University of Karachi, Karachi-75270, Pakistan

[b]Department of Chemistry, University of Karachi, Karachi-75270, Pakistan

SGM: musharraf1977@yahoo.com

QA: quaish_85@yahoo.com

FUH: faraz.ulhaq@iccs.edu

HA: haris_ahmed90@live.com

*Corresponding author. Tel.: +92 213 4824924-5; 4819010; fax: + 92 213 4819018-9.

E-mail address: musharraf1977@yahoo.com

ABSTRACT

Mesterolone is a synthetic androgenic-anabolic steroid (AAS) used for the cure of infertility and hypogonadism. Mesterolone cannot be analyzed by a UV detector because of the lack of a chromophore and this puts limitations on its direct UV analysis. This paper reports development and validation of a simple and cost-effective post-derivatized TLC-densitometric method using ceric sulfate as staining reagent for the analysis of mesterolone and its degraded products under various stress conditions, as recommended in the ICH guidelines. The limit of detection and limit of quantification for mesterolone in this method were found to be 1.64 and 4.97 ng/spot respectively. The current study suggests that mesterolone is very prone to photochemical degradation while quantum chemical calculations carried out as an integral part of this study supplement the assessed reactivity of mesterolone under applied stress conditions. The developed stability-indicating TLC-densitometric method can be employed for analysis of mesterolone in the presence of its degradation products.

Keywords: mesterolone, stress degradation, stability-indicating, TLC-densitometry, quantum chemical calculations

Introduction

Androgenic-anabolic steroids (AAS) are testosterone derived drugs that stimulate protein synthesis resulting in accelerated rate of food consumption, increased muscle growth, body mass and enhanced performance by binding to androgen receptors that maintain male characteristics [1]. The pharmaceutical market has many formulations available that either contains individual steroids or their combinations in various dosage forms. In spite of the fact that World Anti-Doping Agency (WADA), International Olympic Committee (IOC) and other sports authorities have restricted the use of AASs, their self-administration is continuously practiced by many individuals, particularly sportsmen, is a desire to enhance athletic performance, aggressiveness, body strength and shape [2-4]. Mesterolone (1α-methyl-5α-androstan-17*β*-ol-3-one), first synthesized by Wiechert and patented in 1968 [5], is generally used for the cure of infertility and hypogonadism [6, 7] and is one of the most utilized androgenic-anabolic steroids (AAS) by athletes due to its antiestrogenic activity. The analysis of mesterolone, therefore requires much attention because of its presence on the WADA prohibited substances list.

The International Conference on Harmonization (ICH) and Food and Drug Administration (FDA) require stress degradation analysis of drugs to explain the inherent stability characteristics of the active component. These guidelines emphasize to explore features possibly affected by various environmental factors such as light, humidity, oxidation, pH variation and temperature. Validated stability-indicating analysis methods therefore must be employed for quality assurance, safety and efficacy of pharmaceutical formulations. During stress degradation studies, Quantum-chemical calculations can serve as useful tool for prediction of degradation pathways and identification of degradation prone sites in a molecule. These calculations serve their purpose equally well when applied to stability-indicating studies of either drug formulations or

lead molecules in drug discovery. Furthermore, the determination of HOMO (Highest occupied molecular orbital) and LUMO (Lowest unoccupied molecular orbital) size can lead to an estimation of overall reactivity of the molecule using the density of electrons dispersed over these orbitals [8-15].

Various analytical methods based on gas chromatography-mass spectrometry (GC-MS), spectrophotometry and matrix-assisted laser desorption/ionization time-of-flight spectrometry have been previously published for the analysis of mesterolone in different matrices [16-20] however, to the best of our knowledge no method has so far been reported for the photochemical degradation studies and stability indicating TLC-densitometric analysis of mesterolone.

A number of benefits make TLC-densitometry a method of choice for routine chemical analysis. In comparison to HPLC, TLC-densitometry is cost effective and environment friendly as it consumes minimum amount of solvents. This technique offers reduced analysis time by being able to process several samples simultaneously.

In addition to our previous contributions to the development of various chromatographic methods for the analysis of biologically and pharmaceutically important compounds [21-27], this study describes a simple stability-indicating TLC-densitometric method for the analysis of mesterolone in pharmaceutical products as per ICH guidelines[28] and also establishes mesterolone's reactivity under various stress conditions.

Experimental

Standards and chemicals

Mesterolone was purchased from Tokyo Chemical Industry Co., Ltd. Proviron tablets (containing 25 mg mesterolone / tablet manufactured by Bayer Schering Pharma) were procured from local pharmaceutical market in Karachi, Pakistan. Sodium hydroxide (NaOH) was acquired

from BioM Laboratories (Cerritos, USA). Hydrogen peroxide (H_2O_2, 35% v/v) and hydrochloric acid (HCl) were purchased from Fisher Scientific (UK). Precoated silica gel aluminum sheets ($60F_{254}$, 20 cm × 20 cm) were ordered from Merck (Germany). Deionized water used throughout this study was obtained by passing distilled water from Millipore Milli-Q Integral Water Purification System (Bedford, USA). Others solvent required for sample preparation and analysis were purchased from Merck, (Germany).

Instrumentation and computational analysis

Samples were sprayed as bands of 6mm width on precoated silica gel aluminum plate 60 (F_{254}, (20 cm × 10 cm with 0.20 mm layer thickness) by CAMAG automatic TLC sample applicator (Linomat 5) using CAMAG 100 µL glass syringe. A constant application rate of 0.1 µL/s was maintained and two sample bands were separated by a distance of 9.1 mm. Monochromatic bandwidth was set at 20 nm while each track was scanned thrice with baseline correction. Mobile phase composition was hexane:acetone (6.5:3.5 *v/v*) while a total of 10 mL mobile phase was used per chromatographic analysis. Linear ascending development was carried out in CAMAG twin trough glass chamber (20 cm×10 cm) in an unsaturated condition. The chromatographic process was carried out at room temperature (25 ± 2 $^{\circ}$C) with relative humidity 43 ± 5% while the length of run chromatogram was 8 cm. Developed TLC plate was dried for 3-5 minutes using hot air from a hair dryer and subjected to staining process using CAMAG Chromatogram Immersion Device. TLC plate immersed in the staining reagent (Ceric sulfate) was heated for 4-5 minutes at 110-120 ^{o}C on CAMAG TLC Plate Heater 3. Developed TLC plate was scanned at λ_{max} 466 nm on CAMAG TLC Scanner 3 operating in reflection absorbance mode and controlled by winCATS software. Slit dimensions were set at 5 mm × 0.45 mm and scanning speed was 10

mm s^{-1}. Radiation source was a deuterium lamp operating in 190 nm to 400 nm wavelength range and evaluation was carried out *via* peak areas using linear regression analysis.

Quantum chemical calculations were also performed to determine spatial electron distribution on HOMO and LUMO and for initial geometry interpretation of mesterolone. Initial geometry was optimized using Spartan 08 v 1.2.0 (Wavefunction, CA, USA) by means of density functional theory (DFT) method with Becke-3-Le-Yang-Parr (B3LYP) and 6-31G** basis sets on a PC equipped with an Intel® Core™ i3 processor running Microsoft Windows 7 (64-bit edition).

Calibration curve of standard mesterolone

Calibration curve was constructed using six standard solutions prepared by independently weighing mesterolone and making up the individual volumes with methanol. The solutions were stored at 4 °C prior to analysis. Five µL from each standard solution was spotted three times on the TLC plate at various concentrations (200, 400, 600, 800, 1000, and 1200 ng per spot) and subjected to chromatographic analysis. The spotted plate was developed as described in experimental section. The procedure was repeated six times to obtain an average standard calibration curve in the range 200–1200 ng per spot. Residual linearity test was used to verify the linearity of standard calibration curve.

Method validation

ICH guidelines were followed throughout method validation process. Sensitivity of the method was determined with respect to LOD, LOQ and correlation coefficient. Linearity was evaluated by spotting 5 µL from each dilution three times on the TLC plate to give concentration range of 200-1200 ng per spot and subjected to chromatographic analysis. The limit of detection (LOD) and limit of quantification (LOQ) were estimated at 3 and 10 times of the noise level. Moreover, LOD and LOQ were also experimentally confirmed by diluting the known concentrations of

mesterolone till the average instrumental responses were approximately 3 and 10 times of the standard deviation of the responses for six replicates. Method precision was determined by intra- and inter-day analyses of mesterolone for repeatability and reproducibility. This was achieved by spotting three different concentrations (300, 500 and 700 ng/spot) on the TLC plate. Repeated analyses were performed on the same day for the intra-day analysis and on the next day for inter-day analyses. Results were listed as percent relative standard deviation (% R.S.D.). Robustness was assessed by deliberately varying different parameters within the range of ± 5% at three different concentration levels such as using different types of TLC plates e.g., silica-gel glass plates and aluminum sheets procured from other supplier (Macherey-Nagel, Germany), varying mobile phase composition, varying time from spotting to chromatography, varying time from chromatography to derivatization, varying time for derivatization and varying time from derivatization to scanning. Recovery studies were carried out on pre-analyzed samples for the assessment of method accuracy by spiking with extra 50, 100 and 150% standard mesterolone. This procedure was also followed in six replicates.

Forced degradation study of mesterolone

50 mg of mesterolone was dissolved in 50 mL of methanol to achieve 1 $mg.mL^{-1}$ solution which was used for each experiment. Stress degradation studies were performed using parallel sixteen reaction vessels synthesizer (Smart Start Synthesizer, Chem Speed Ltd., Switzerland).

3 mL of stock solution of mesterolone (1 $mg.mL^{-1}$) was mixed with 3 mL of each 0.1N, 1N and 5N NaOH independently for alkaline hydrolysis and the consequential blends were refluxed at 80 ^{o}C for two hours in the dark to avoid any possible photodegradation of the compound. For neutral hydrolysis, 3 mL of methanolic stock solution was mixed with 3 mL of milli Q water and refluxed for two hours in the dark. For the experiment of acidic hydrolysis, 3 mL of methanolic

stock solution of mesterolone was mixed with 3 mL of each 0.1 N, 1N and 5N HCl independently for acidic hydrolysis and the consequential blends were refluxed at 80 ^{o}C for two hours in the dark. For thermal degradation, 3 mL of methanolic stock solution of mesterolone was refluxed at 80 ^{o}C for two hours in the dark. Experiment on the oxidation degradation was carried out by mixing 3 mL of the stock solution with 3 mL of H_2O_2 (35% v/v) and refluxed at 80 ^{o}C for two hours in dark.

Photochemical stability of mesterolone was studied by exposure of powdered mesterolone to direct sunlight for seven days at 30 ± 2 ^{o}C from 09:00 am to 05:00 pm. 1 mg of sunlight exposed mesterolone was dissolved in 2 mL of methanol to give stock solution for the treated standard. Powdered mesterolone was stored in oven for 4 hrs at 90 ^{o}C for dry heat-induced degradation. Stock solution for dry heat exposed mesterolone was prepared by dissolving 1 mg of treated standard in 2 mL of methanol. 3 mL methanolic stock solution of mesterolone was mixed with 3 mL of H_2O_2 (35% v/v) kept for 24 hours for hydrogen peroxide induced oxidation at room temperature. 2 µL (1000 ng/spot) each of alkali treated solutions, neutral hydrolysis solutions, acid treated solutions, oxidation degraded solution, dry heat-treated solution, light exposed solution, hydrogen peroxide induced oxidized mesterolone solution and wet heated solutions were applied on TLC plates in triplicate and the densitograms were developed as described in experimental section.

Analysis of marketed drug formulation

A total of 20 mesterolone tablets (label claim: 25 mg mesterolone per tablet) were accurately weighed and powdered with the help of mortar and pestle for 3-5 minutes. 10 mg of the homogenized powder was accurately weight and transferred to a volumetric flask containing 10 mL methanol. The mixture was sonicated for 10 minutes to ensure complete extraction of

mesterolone from the tablet matrix. The resulting solution was filtered and 2 mL of it were diluted to 10 mL with methanol. 5 µL (1000 ng $spot^{-1}$) of the diluted solution was applied on TLC sheet followed by development, staining and scanning.

ESI-QqTOF-MS/MS analysis of photo-degraded products

The standard mesterolone and its photo-degraded products were collected from the spots separated from the TLC plate and dissolved in methanol. Working dilution was prepared in a mixture of 1:1 acetonitrile and water, containing 0.1% formic acid. Analysis was performed by electrospray ionization (ESI) and collision-induced dissociation (CID), positive ion mode, on a tandem mass spectrometer (QSTAR XL mass spectrometer Applied Biosystems/MDS Sciex, Darmstadt, Germany) coupled with Agilent 1100 HPLC system. High purity nitrogen gas was used as the curtain gas and collision gas (generated using Peak Scientific nitrogen generator). The ESI interface conditions were as follows: ion spray capillary voltage of 5500 V, curtain gas flow rate 20 L min^{-1}, nebulizer gas flow rate 30 L min^{-1}, DP1 60 V, DP2 10 V, and focusing potential of 265 V. The collision energy was swept from 20 to 45 eV for MS/MS experiment. Samples were introduced into the mass spectrometer using a Harvard syringe pump (Holliston, MA) at a flow rate of 5 µL min^{-1}.

Results and discussion

Optimization of method

The purpose of chromatography was to develop a stability-indicating method for mesterolone. Solutions containing standard mesterolone and its degraded products were spotted on TLC plates and developed in various mobile phases. Different solvents system were tried to separate mesterolone from its degraded products in good resolution. Peak widths and R_f values of mesterolone in different solvent systems are listed in Table 1. Best results were obtained when

the mobile phase was a 6.5:3.5 v/v mixture of hexane and acetone in unsaturated condition (Figure. 1A). Peak for mesterolone appeared at R_f = 0.53 ± 0.03 while peaks for its photodegradation products (D1 and D2) appeared at R_f = 0.46 and R_f = 0.67, respectively. Staining reagents like phosphomolybdic acid (PMA), ceric sulfate, ceric ammonium sulfate and vanillin were tried for derivatization while best results were obtained with ceric sulfate staining. Spots stained with ceric sulfate were brighter and sharper than with other derivatization agents.

Six different concentrations of mesterolone (200, 400, 600, 800, 1000 and 1200 ng/spot), prepared in methanol, were simultaneously spotted in triplicate on aluminum TLC plates and developed as described in experimental section. Peak area and concentration were subjected to least squares linear regression analysis to calculate the calibration equation and correlation coefficient. The linear regression data for the calibration curves (n = 6) showed linearity (r = 0.9967 ± 0.002) over the range of 200-1200 ng /spot. In the residual linearity test, a random pattern of residuals versus applied standard concentrations showed linear model for standard calibration curve.

Method validation

The repeatability of the sample analysis was assessed and tabulated as percentage relative standard deviation (R.S.D.) between two analyses and was found to be less than 1% when performed by two different analysts. Similarly, intra- and inter-day analysis of mesterolone was found to be reproducible as the R.S.D. was less than 1% (Supplementary file 1). For the assessment of robustness of our developed method, % R.S.D. was calculated for three different criteria as the concentration was varied (300, 500 and 700 ng). Average %R.S.D. was 0.62 for change in solvent composition, 0.48 for varying TLC plates, 0.62 for varying time from spotting to chromatography, 0.49 for varying time duration for chromatography to staining, and 0.48 for

duration for staining and 0.6 for varying time duration from staining to scanning (Supplementary file 2). RSD % was found to be less than 1.5% for every criterion which shows that the developed method is reasonable robust. This method was found to be sensitive as LOD for standard mesterolone at signal/noise ratio of 3:1 was found to be 1.64 ng per spot while LOQ at signal/noise ratio 10:1 was found to be 4.97 ng/spot. To check the peak purity of mesterolone the spectra were compared at peak start, peak apex and peak end positions of the spot. Good correlation, r^2 (start to middle) = 0.9997 and r^2 (middle to end) = 0.9996 were obtained between standard and sample spectra of mesterolone. The recovery of the method was found to be 97.5–99.2% after spiking with 50, 100 and 150% of additional standard mesterolone (Supplementary file 3). All of the validation parameters have been summarized in Table 2.

Analysis of pharmaceutical product

The chromatogram of mesterolone extracted from tablets afforded a compact spot at $R_f = 0.53 \pm 0.03$ while no interference was observed from the excipients generally added in tablet formulations (Figure. 1B). Mesterolone content of the tablet was found to be 24.847 ± 0.304 mg (99.39 %) with an R.S.D. of 1.22%. This low % R.S.D. value indicates the usefulness of this method for usual analysis of mesterolone in pharmaceutical products.

Stability indicating property of mesterolone

The chromatogram for light exposed sample of mesterolone showed additional peaks for two degradation products at R_f = 0.46 (D1) and R_f = 0.67 (D2), respectively. The spots for degradation products were well resolved from the standard mesterolone spot as shown in Figure. 1C. On the other hand, samples degraded under acid, base, heat and oxidation conditions showed no additional peaks. Table 3 shows the R_f values of degradation products and the percent degradation of mesterolone under the mentioned stress conditions.

Current stability indicating assay of mesterolone was also aided by computational calculations of HOMO and LUMO. These calculations led to the explanation of observed degradation of mesterolone under different conditions. Mesterolone was found to be quite stable under thermal degradation conditions and this can be explained by its calculated values of enthalpy (-2429219.48 kJ/mol) and free energy (-2429399.48 kJ/mol). These values suggest a high thermodynamic stability for mesterolone and hence it does not degrade even under accelerated thermal conditions. It was seen from the calculation results that the HOMO is spread from the methyl group of C-1 to C-4 suggesting the presence atomic centers vulnerable to electrophilic attack in this region. In principle, acidic conditions should result in protonation in this region which should not lead to any substantial degradation of the molecule. This assumption was supported by our experimental findings where only 1 – 4 % degradation under acidic conditions was observed. The LUMO orbital was found to be spread in the region from C-2 to C-4 which is the enolizable region. However, the mesterolone molecule owing to its high thermodynamic stability does not undergo aldol type reactions. This was again supported by experimental data where only 1 – 5 % degradation under alkaline conditions was observed. If the findings from the HOMO and LUMO calculations are combined (Figure. 2), the observation of two photodegradation products (D1 and D2) can be explained. The formation of D1 is probably due to cleavage of the bond between C-2 and C-3. Photo-degraded product D2 was found to be a dimer of mesterolone which is probably dimerized by an enolate formation at C-2 and the attack of enolate on the C-3 of other molecule. The thermodynamic stability of the molecule may have a role in these findings as UV light can provide energy required for the molecule to undergo such type of reactions.

The elemental compositions of both photo-degraded products were determined by precise mass measurements from the ESI-QqTOF-MS. ESI-QqTOF-MS (positive mode) scan of mesterolone and its degraded products showed the peaks of $[M+H]^+$ at *m/z* 305.2497 (MS), 337.2743 (D1) and 591.4780 (D2) corresponding to the molecular formulae $C_{20}H_{33}O_2^+$ (calc. 305.2475), $C_{21}H_{37}O_3^+$ (calc. 337.2737) and $C_{40}H_{63}O_3^+$ (calc. 591.4771), respectively. MS/MS spectra of standard mesterolone and its photo-degraded products are provided in Figure. 3. Elemental compositions of both photo-degraded products are listed in Table 4.

Conclusion

The current study establishes the intrinsic stability of mesterolone under various stress conditions. Of all the stress conditions investigated, mesterolone was found to be most susceptible to photochemical degradation. Two photo degraded products were observed with significantly different R_f values. The developed stability-indicating TLC densitometric method was found to be rapid, accurate and precise and can be efficiently used for the direct identification and quantification of mesterolone in its pharmaceutical formulations. The computational calculations also provided a clear understanding of mesterolone reactivity under photochemical conditions. In addition, the characterization of photo-degraded products will be useful for the better understanding of degradation pathways.

Competing interests

The authors declare that they have no competing interests.

Acknowledgements

The authors are grateful to the PAS (Pakistan Academy of Sciences) for financial support (Project Reference No. 5-9/PAS/54).

Supplementary Material

The following supplementary files are available with the online version of this paper in pdf format.

Supplementary file 1. Precision and accuracy for quality control standard of mesterolone

Supplementary file 2. Robustness testing (n = 6)

Supplementary file 3. Recovery studies (n = 6)

Figure and Table Legends

Figure. 1. TLC chromatogram of standard mesterolone (1000 ng/ spot), R_f = 0.53 ± 0.03 (**a**), TLC Chromatogram of pharmaceutical product Proviron (**b**), chromatogram of photo degraded mesterolone (1000 ng/ spot), degradant (D1) has R_f = 0.46 and degradant (D2) has R_f = 0.67 (**c**): mobile phase; hexane: acetone (6.5:3.5, *v/v*)

Figure. 2. Optimized molecule geometry (**a**), LUMO (**b**) and HOMO (**c**) orbitals of mesterolone

Figure. 3. Product ion spectra of mesterolone (A) and its photo-degraded products D1 (B), D2, at collision energy of 25 eV.

Table 1. R_f values and peak widths of mesterolone in different mobile phases

Table 2. Summary of validation parameters

Table 3. Summary of stress degradation studies of mesterolone

Table 4. Elemental composition of the Photo-degraded products of mesterolone.

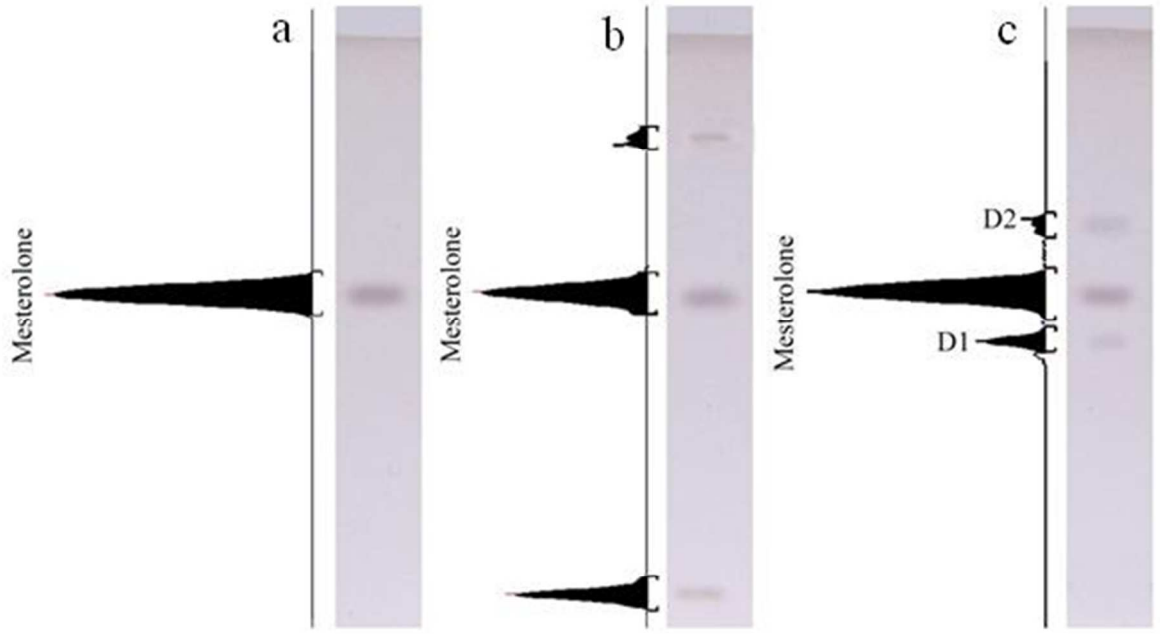

Figure. 1. TLC chromatogram of standard mesterolone (1000 ng/ spot), R_f = 0.53 ± 0.03 (**a**), TLC Chromatogram of pharmaceutical product Proviron (**b**), chromatogram of photo degraded mesterolone (1000 ng/ spot), degradant (D1) has R_f = 0.46 and degradant (D2) has R_f = 0.67 (**c**): mobile phase; hexane: acetone (6.5:3.5, *v/v*)

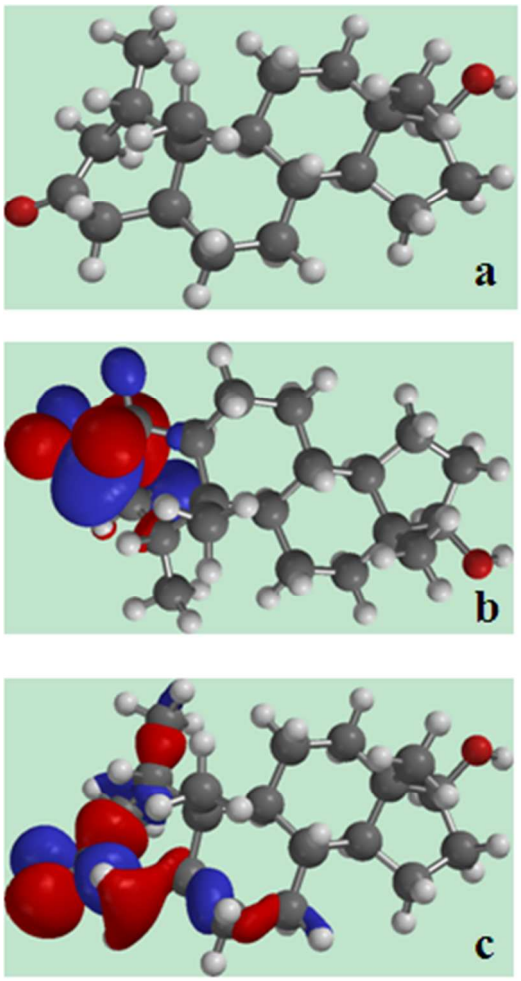

Figure. 2. Optimized molecule geometry (**a**), LUMO (**b**) and HOMO (**c**) orbitals of mesterolone

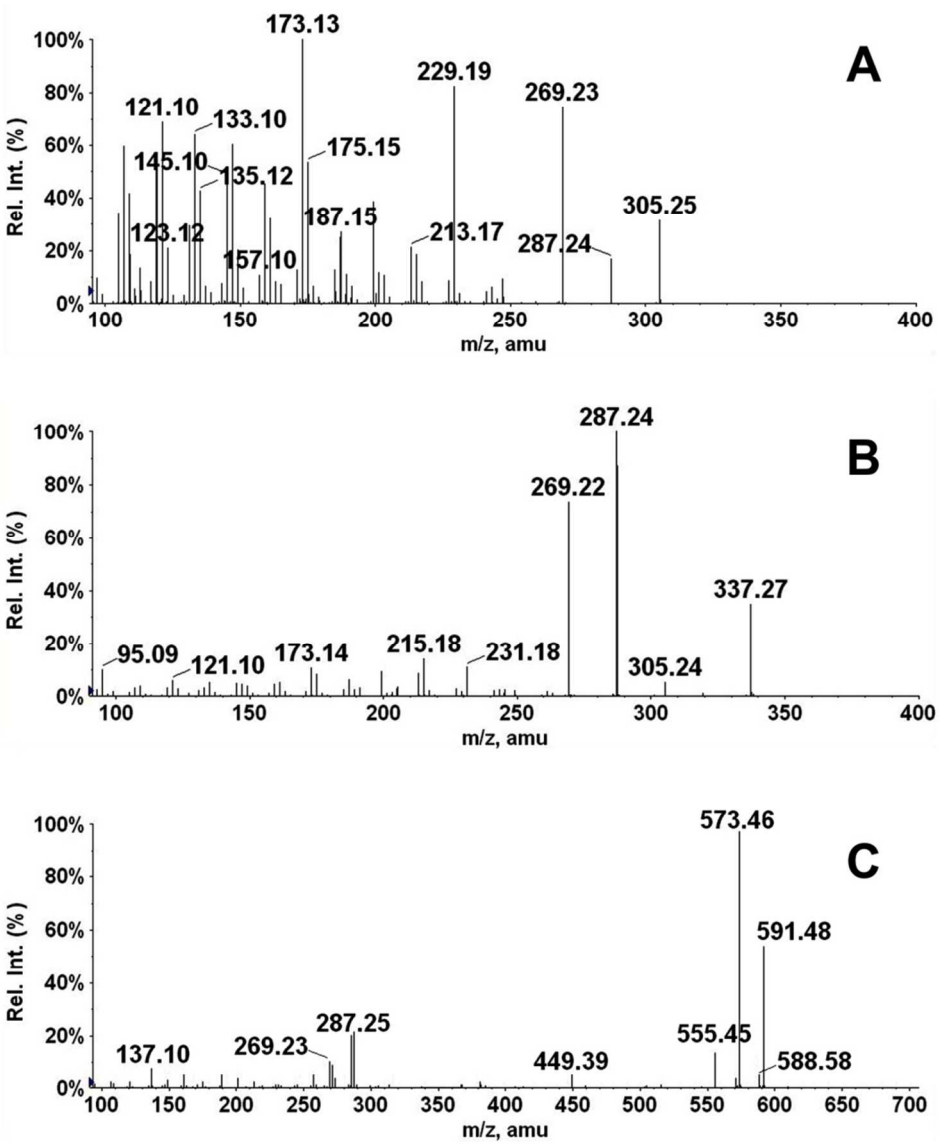

Figure. 3. Product ion spectra of mesterolone (A) and its photo-degraded products D1 (B), D2, at collision energy of 25 eV.

Table 1. R_f values and peak widths of mesterolone in different mobile phases

S. No	Solvent Composition	Proportion(*v/v*)	Retention Factor R_f	Peak Width ΔR_f(cm)
1	Hexane-ethyl acetate	8:2	0.19	0.08
2	Chloroform-methanol	9.4:0.6	0.21	0.11
3	Dichloromethane-methanol	9.2:0.8	0.14	0.07
4	Hexane-acetone	6:4	0.57	0.07
5	Hexane-acetone	6.5:3.5	0.53	0.06
6	Hexane-acetone	7:3	0.45	0.07

Table 2. Summary of validation parameters

Parameter	Data of standard mesterolone (at λ_{max} 466 nm)
Linearity range	200-1200 ng/spot
Correlation coefficient	0.9967 ± 0.002
Limit of detection (LOD)	1.64 ng/spot
Limit of quantification (LOQ)	4.97 ng/spot
Y = mx + c	Y = 7.28X + 525.49
Slope ± SD	7.28 ± 0.32
Intercept ± SD	525.49 ± 3.528
Intra-day analysis (n=3), % R.S.D.	0.367
Inter-day analysis (n=3), % R.S.D.	0533
Robustness	Robust
Specificity	Specific

Table 3. Summary of stress degradation studies of mesterolone

Degradation conditions	% Recovery	% Degradation	R_f of degraded products
Acidic hydrolysis [a]			
0.1N HCl	98.27	1.73	Not detected
1N HCl	97.35	2.65	Not detected
5N HCl	95.47	4.53	Not detected
Basic hydrolysis [a]			
0.1N NaOH	98.32	1.68	Not detected
1N NaOH	96.59	3.41	Not detected
5N NaOH	94.61	5.39	Not detected
Neutral hydrolysis [a]	98.53	1.47	Not detected
Wet heating [a]	98.46	1.54	Not detected
Dry heating	97.62	2.38	Not detected
Oxidation [a]			
5%v/v H_2O_2	98.69	1.31	Not detected
35%v/v H_2O_2	95.43	4.57	Not detected
Oxidation at room temp	98.83	1.17	Not detected
Photostability-daylight	82.57	17.43	0.46, 0.67

[a]Reflux in parallel synthesizer for two hours at 80 °C

Table 4. Elemental composition of the photo-degraded products of mesterolone.

Product ID	Proposed formula	Observed mass	Calculated mass	Error (ppm)
MS	$C_{20}H_{33}O_2^+$	305.2497	305.2475	7.1842
D1	$C_{21}H_{37}O_3^+$	337.2743	337.2737	1.7142
D2	$C_{40}H_{63}O_3^+$	591.4780	591.4771	1.3984

References

1. J. L. Donahue and D. T. Lowenthal, *Am J Ther*, 2000, **7**, 365-373.
2. P. Aagaard and J. L. Andersen, *Scand J Med Sci Sports*, 2010, **20 Suppl 2**, 39-47.
3. P. A. Harmer, *Br J Sports Med*, 2010, **44**, 26-31.
4. M. W. Kibble and M. B. Ross, *Clin Pharm*, 1987, **6**, 686-692.
5. W. Rudolf, *Journal*, 1968.
6. G. Corona, L. Vignozzi, A. Sforza and M. Maggi, *World J Mens Health*, 2013, **31**, 103-125.
7. B. N. Barwin, S. D. Clarke, J. D. Biggart and A. Lamont, *Practitioner*, 1973, **211**, 669-674.
8. J. Aihara and M. Yoshida, *J Mol Graph Model*, 2001, **19**, 194-198.
9. M. Arivazhagan and D. Anitha Rexalin, *Spectrochim Acta A Mol Biomol Spectrosc*, 2013, **107**, 347-358.
10. M. Arivazhagan and D. Anitha Rexalin, *Spectrochim Acta A Mol Biomol Spectrosc*, 2013, **104**, 451-460.
11. M. Arivazhagan and S. Jeyavijayan, *Spectrochim Acta A Mol Biomol Spectrosc*, 2011, **79**, 376-383.
12. M. Arivazhagan, S. Jeyavijayan and J. Geethapriya, *Spectrochim Acta A Mol Biomol Spectrosc*, 2013, **104**, 14-25.
13. M. Arivazhagan, R. Meenakshi and S. Prabhakaran, *Spectrochim Acta A Mol Biomol Spectrosc*, 2013, **102**, 59-65.
14. M. Arivazhagan, S. Prabhakaran and R. Gayathri, *Spectrochim Acta A Mol Biomol Spectrosc*, 2011, **82**, 332-339.
15. M. Arivazhagan, V. P. Subhasini and A. Austine, *Spectrochim Acta A Mol Biomol Spectrosc*, 2012, **86**, 205-213.
16. E. N. Ho, D. K. Leung, G. N. Leung, T. S. Wan, H. N. Wong, X. Xu and J. H. Yeung, *Anal Chim Acta*, 2007, **596**, 149-155.
17. D. de Boer, E. G. de Jong, R. A. Maes and J. M. van Rossum, *J Steroid Biochem Mol Biol*, 1992, **42**, 411-419.
18. R. Masse and D. Goudreault, *J Steroid Biochem Mol Biol*, 1992, **42**, 399-410.

19. D. Zivanov-Stakic, L. J. Milosevic and D. Agbaba, *J Pharm Biomed Anal*, 1989, **7**, 1893-1896.
20. M. Galesio, C. Núñez, M. S. Diniz, R. Welter, C. Lodeiro and J. Luis Capelo, *Talanta*, 2012, **100**, 262-269.
21. S. G. Musharraf, N. Iqbal, U. Gulzar, A. Ali, M. I. Choudhary and R. Atta Ur, *Journal of pharmaceutical and biomedical analysis*, 2011, **56**, 240-245.
22. S. G. Musharraf, N. Iqbal, M. A. Ahmed, S. Mazhar and M. I. Choudhary, *J Liq Chromatogr R T*, 2011, **34**, 2103-2117.
23. S. Musharraf, Q. Arfeen and M. Shoaib, *JPC - Journal of Planar Chromatography - Modern TLC*, 2012, **25**, 331-337.
24. S. G. Musharraf, U. Fatima and R. Sultana, *Chemistry Central journal*, 2012, **6**, 7.
25. S. G. Musharraf and U. Gulzar, *Chemistry Central journal*, 2012, **6**.
26. S. G. Musharraf, N. Kanwal and Q. U. Arfeen, *Chemistry Central journal*, 2013, **7**, 9.
27. S. G. Musharraf, Q. U. Arfeen, W. Mazhar and N. Kanwal, *Chem Cent J*, 2013, **7**, 142.
28. *ICH Q2 (R1) Validation of Analytical Procedures: Text and Methodology*, 2010.

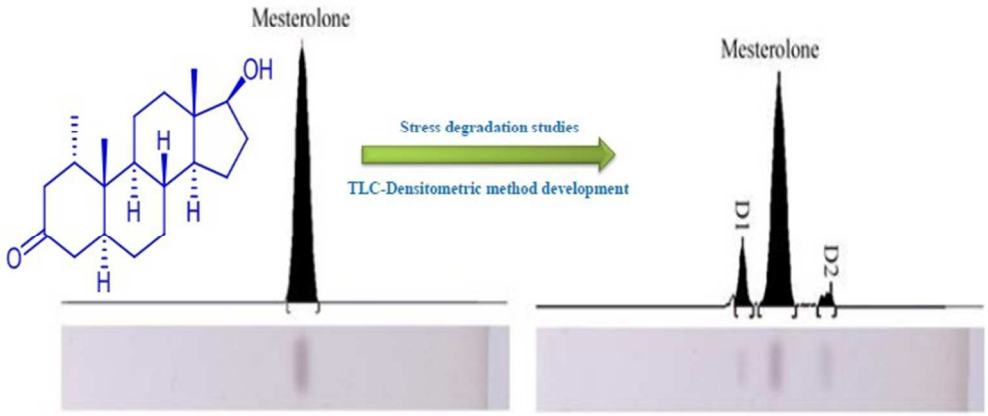

194x101mm (96 x 96 DPI)